Results from angular analyses of B meson decays in CMS

Alessio Boletti (LIP, Lisbon)
on behalf of the CMS Collaboration

9 July 2022 – ICHEP 2022 (Bologna)

Outline

- Introduction
- $B^0 \to K^*(892)^0 \mu\mu$ analysis on Run 1 data [PLB 753 (2016) 424] [PLB 781 (2018) 517]
- $B^+ \to K^+ \mu\mu$ analysis on Run 1 data [PRD 98 (2018) 112011]
- $B^+ \to K^*(892)^+ \mu\mu$ analysis on Run 1 data [JHEP 04 (2021) 124]
- $B^0 \to K^*(892)^0 \mu\mu$ extrapolation to HL-LHC [CMS-PAS-FTR-18-033]

b → sll decays

b → sll decays are an excellent laboratory to probe new physics phenomena:

- **Suppressed in SM** (FCNC, forbidden tree-level)
- NP phenomena can affect BR or angular distributions of final state

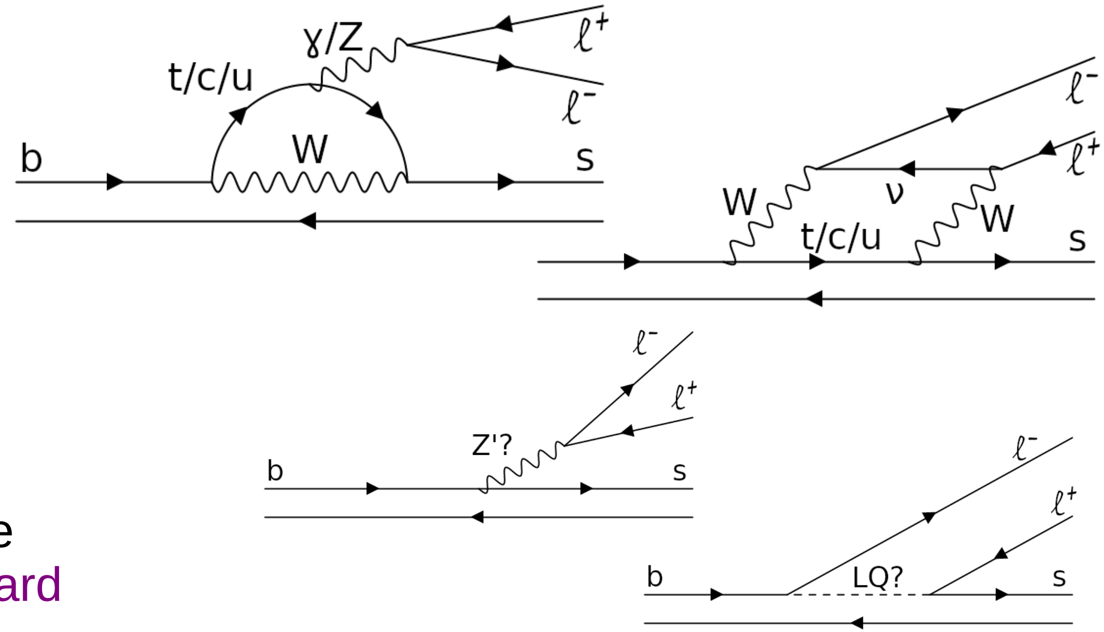

Pseudoscalar **$B^+ \to K^+ \mu\mu$ decay**

- muon direction defines one angular variable
- allows measuring the muon forward-backward asymmetry

Vector-state **$B \to K^*\mu\mu$ decays**

- muon direction and K* polarisation define three helicity angles
- allows measuring a large set of angular parameters, sensitive to EFT coefficients

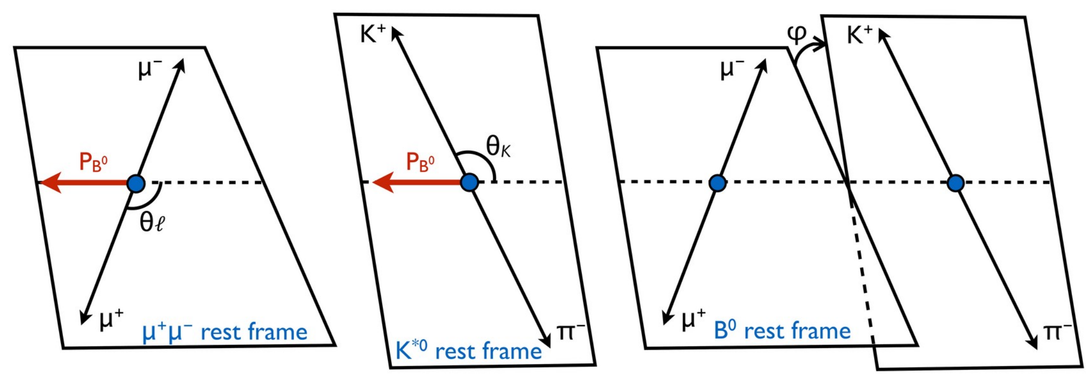

Global fit

- **Tensions with SM predictions** have been observed in one angular parameter, **P'_5**, in $B^0 \to K^{*0} \mu\mu$ decay

$$\frac{d^3\Gamma}{d\cos\theta_l \, d\cos\theta_K \, d\phi} = \frac{9}{32\pi}\Big[\frac{3}{4}F_T\sin^2\theta_K + F_L\cos^2\theta_K + (\frac{1}{4}F_T\sin^2\theta_K - F_L\cos^2\theta_K)\cos 2\theta_l + \frac{1}{2}P_1 F_T \sin^2\theta_K \sin^2\theta_l \cos 2\phi + 2P_2 F_T \sin^2\theta_K \cos\theta_l - P_3 F_T \sin^2\theta_K \sin^2\theta_l \sin 2\phi + \sqrt{F_T F_L}(\frac{1}{2}P'_4 \sin 2\theta_K \sin 2\theta_l \cos\phi + P'_5 \sin 2\theta_K \sin\theta_l \cos\phi) - \sqrt{F_T F_L}(P'_6 \sin 2\theta_K \sin\theta_l \sin\phi - \frac{1}{2}P'_8 \sin 2\theta_K \sin 2\theta_l \sin\phi)\Big]$$

- Set of **coefficients of the effective Hamiltonian** of b-s-l-l vertex (Wilson coefficients) can be derived from measurements of angular parameters

- This allows comparing and combining results from different decays (including BR, LFU, and B_s->ll)

Run 1 results

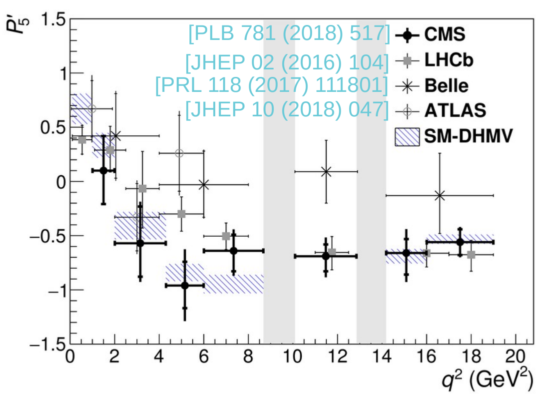

+ partial run 2 LHCb

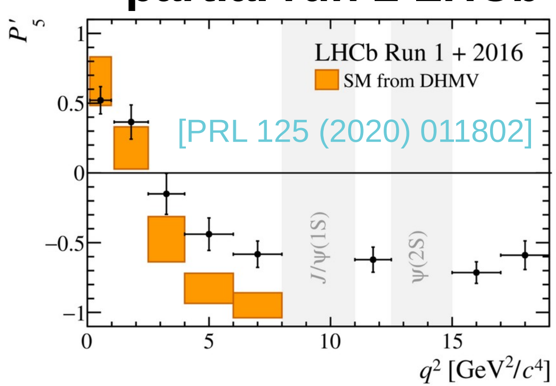

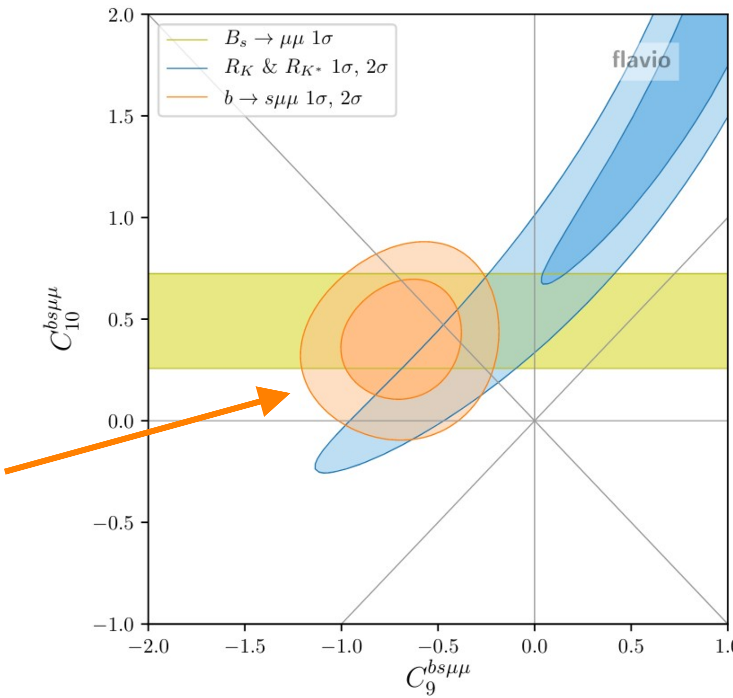

Angular analysis of B→Kμμ decays at CMS

- Analyses performed as a function of the **dimuon invariant mass squared, q^2**, whose spectrum is divided in bins
- **Resonant decays** used as normalisation and control channels:
  - $B \to K\, J/\psi\ (\to \mu\mu)$
  - $B \to K\, \psi(2S)\ (\to \mu\mu)$
- Parameter of interest extracted through **fits** to distributions of **B-candidate mass** and **angular variables**
- Analyses share same two-muon trigger, collecting data in 2012 run

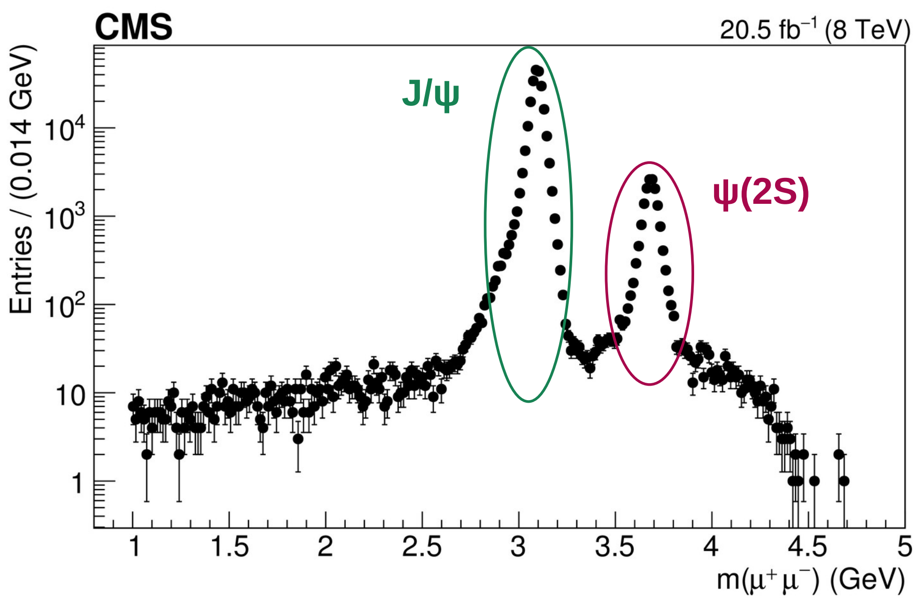

- Effects of detector acceptance and reconstruction and selection efficiency described as function of angular variables and included in the fit PDF
- Statistical uncertainty extracted with profiled Feldman-Cousins procedure
  - ensuring that measurements are robust to borders of physical region of parameter space

$B^0 \to K^{*0} \mu\mu$ angular analysis

[PLB 753 (2016) 424]
[PLB 781 (2018) 517]

Analysis of $B^0 \to K^{*0} \mu\mu$ decay had **two iterations**:

- The first one integrated over the ϕ angle, resulting in a 3D fit to measure branching ratio, forward-backward asymmetry, A_{FB}, and fraction of longitudinally polarized kaons, F_L
- The second one used a 4D fit to all variables, and applied the variable folding to measure P_1 and P'_5 parameters

K^{*0} reconstructed in decay to $K^+\pi^-$

Main challenges deriving from:

- Integrating events with wrong $K\pi$ mass assignment (~13%) in PDF
- Accurate description of efficiency with 3D function

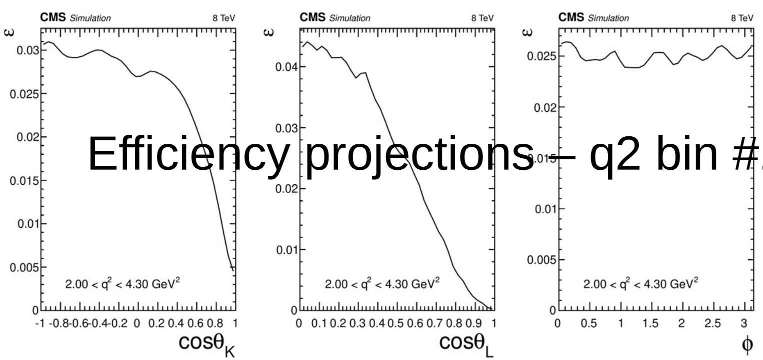

Efficiency projections – q2 bin #1

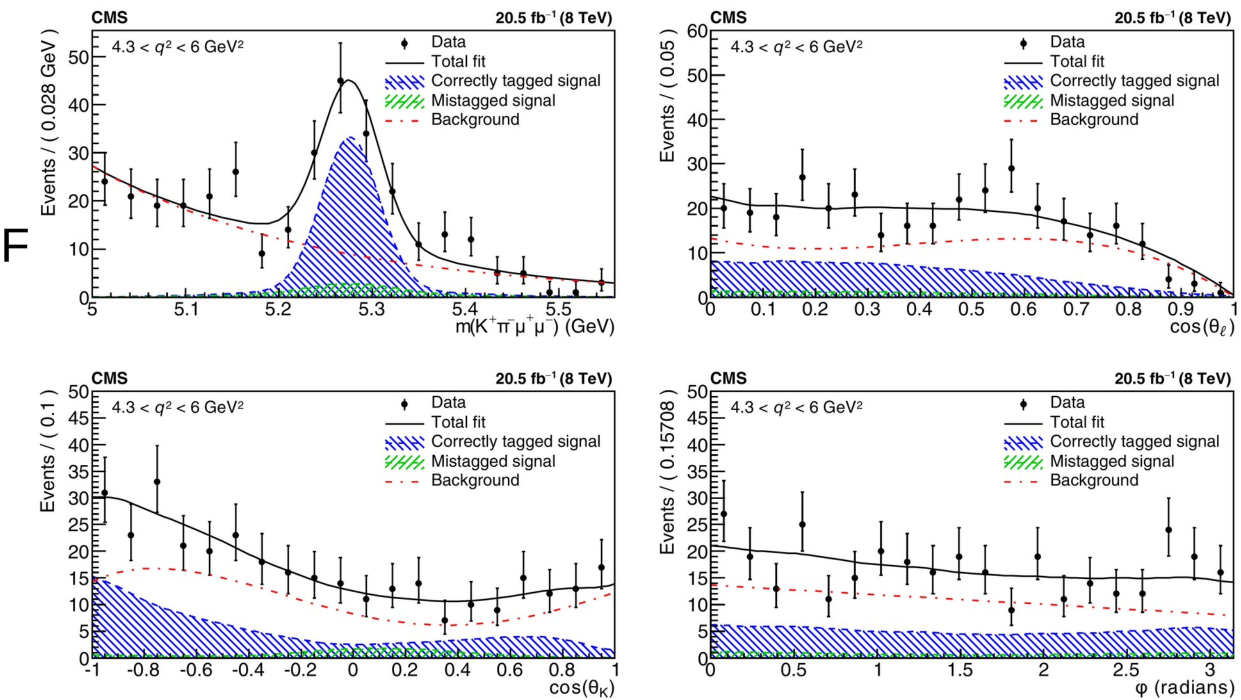

$B^0 \to K^{*0} \mu\mu$ results

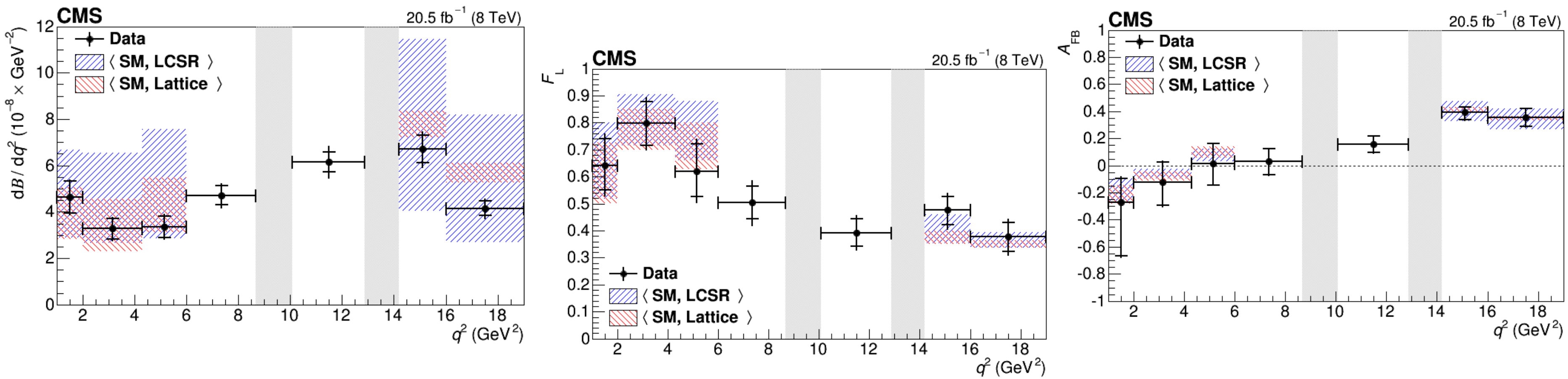

Predictions: [JHEP 07 (2010) 098] [PRD 87 (2012) 034016]

Results are **limited by statistical uncertainty** (internal error bar)

Compatible with Standard Model

Intense scrutiny of P'_5 result, for which other experiments saw tensions with SM

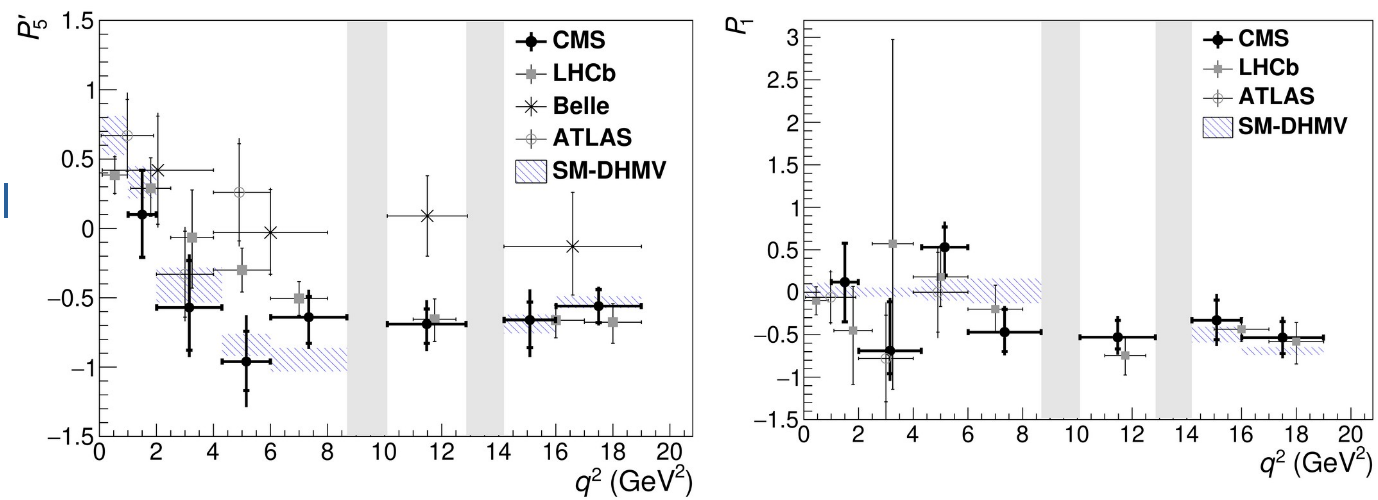

Predictions: [JHEP 01 (2013) 048] [JHEP 05 (2013) 137]

$B^+ \to K^+ \mu\mu$ angular analysis

[PRD 98 (2018) 112011]

Two parameter of interest extracted using 2D fit:
F_H and **A_{FB}**

Analysis performed in 7 bins of q^2, plus two special inclusive ranges (clean q^2 region, full signal region)

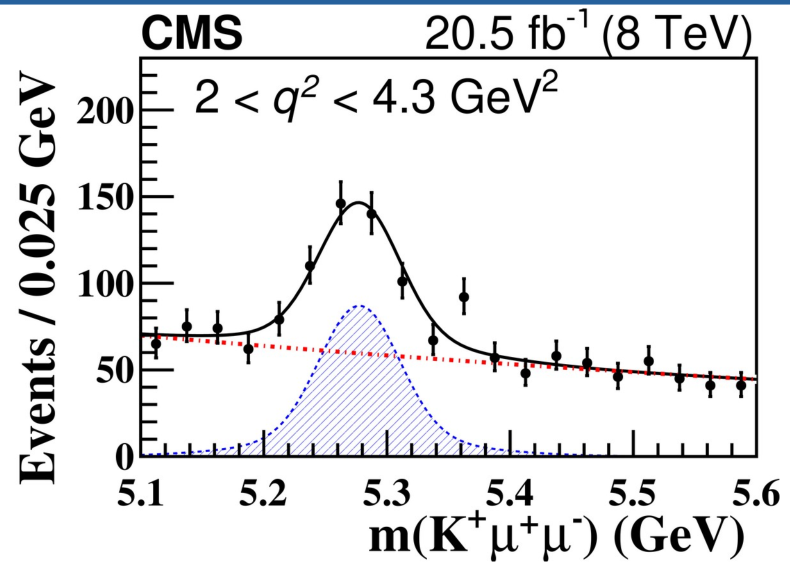

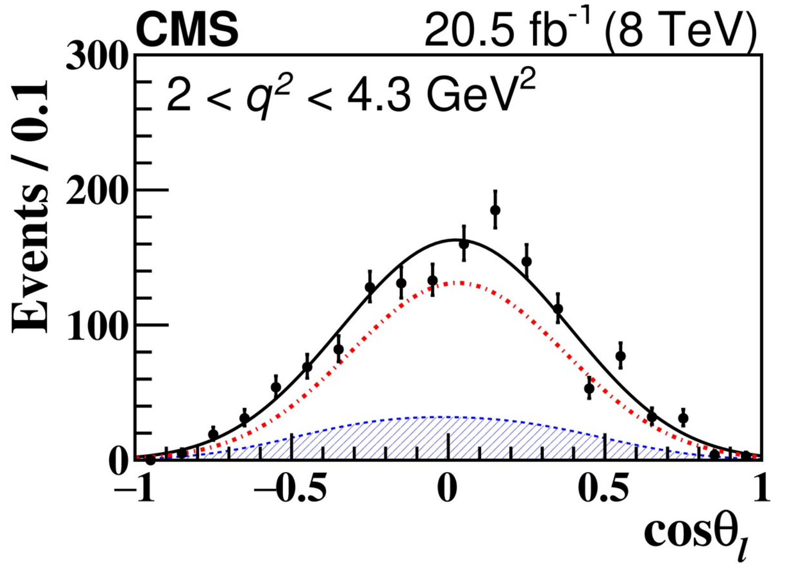

Dominant systematic uncertainty from fitting procedure and description of the background shape

Systematic uncertainty	A_{FB} ($\times 10^{-2}$)	F_H ($\times 10^{-2}$)
Finite size of MC samples	0.4–1.8	0.9–5.0
Efficiency description	0.1–1.5	0.1–7.8
Simulation mismodeling	0.1–2.8	0.1–1.4
Background parametrization model	0.1–1.0	0.1–5.1
Angular resolution	0.1–1.7	0.1–3.3
Dimuon mass resolution	0.1–1.0	0.1–1.5
Fitting procedure	0.1–3.2	0.4–25
Background distribution	0.1–7.2	0.1–29
Total systematic uncertainty	1.6–7.5	4.4–39

$B^+ \to K^+ \mu\mu$ results

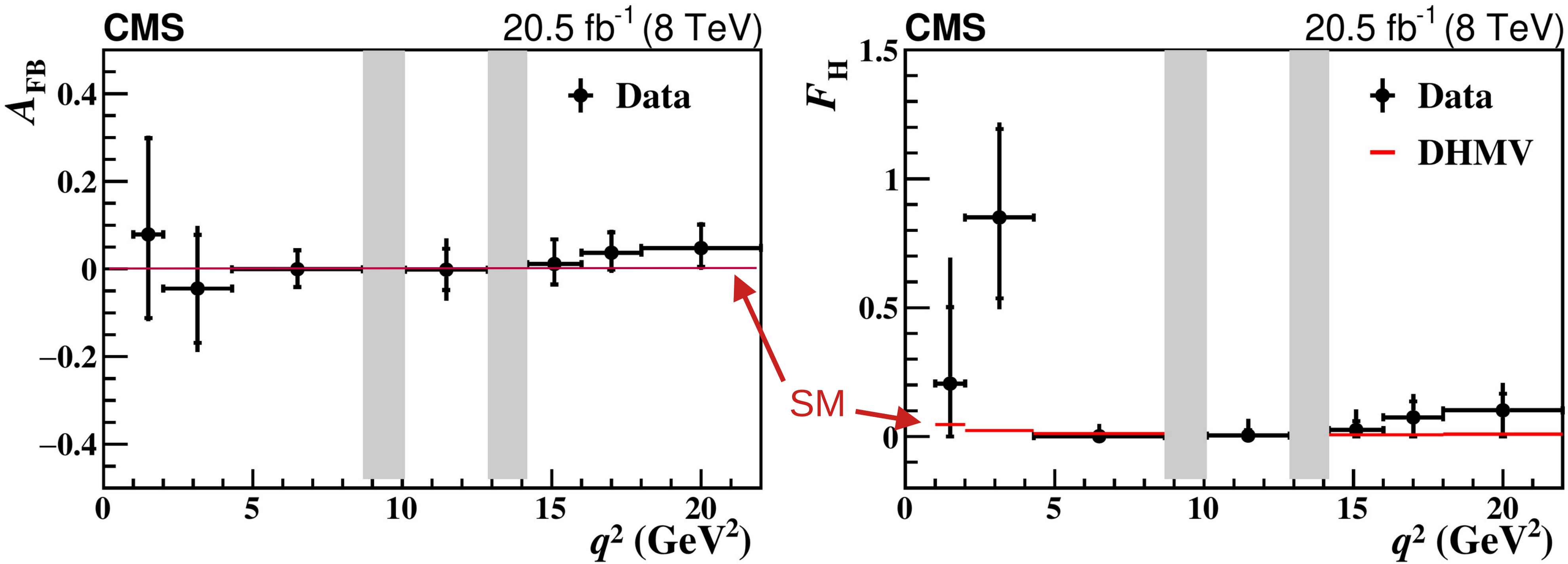

Result dominated by statistical uncertainty in most q^2 bins (inner error bar)

No strong tensions observed with Standard Model predictions ([JHEP 12 (2014) 125], [JHEP 06 (2016) 092])

$B^+ \to K^{*+} \mu\mu$ angular analysis

[JHEP 04 (2021) 124]

3D fit to candidate's **mass** and **two angles**
- Angle ϕ integrated out to simplify fit
- **F_L** and **A_{FB}** measured

Efficiency affected by
challenging K^{*+} reconstruction:
- in K^0_S ($\to$ displaced $\pi^+\pi^-$) and soft π^+
- resulting in lower yield
  wrt neutral decay channel

Analysis performed in 3 bins of q^2

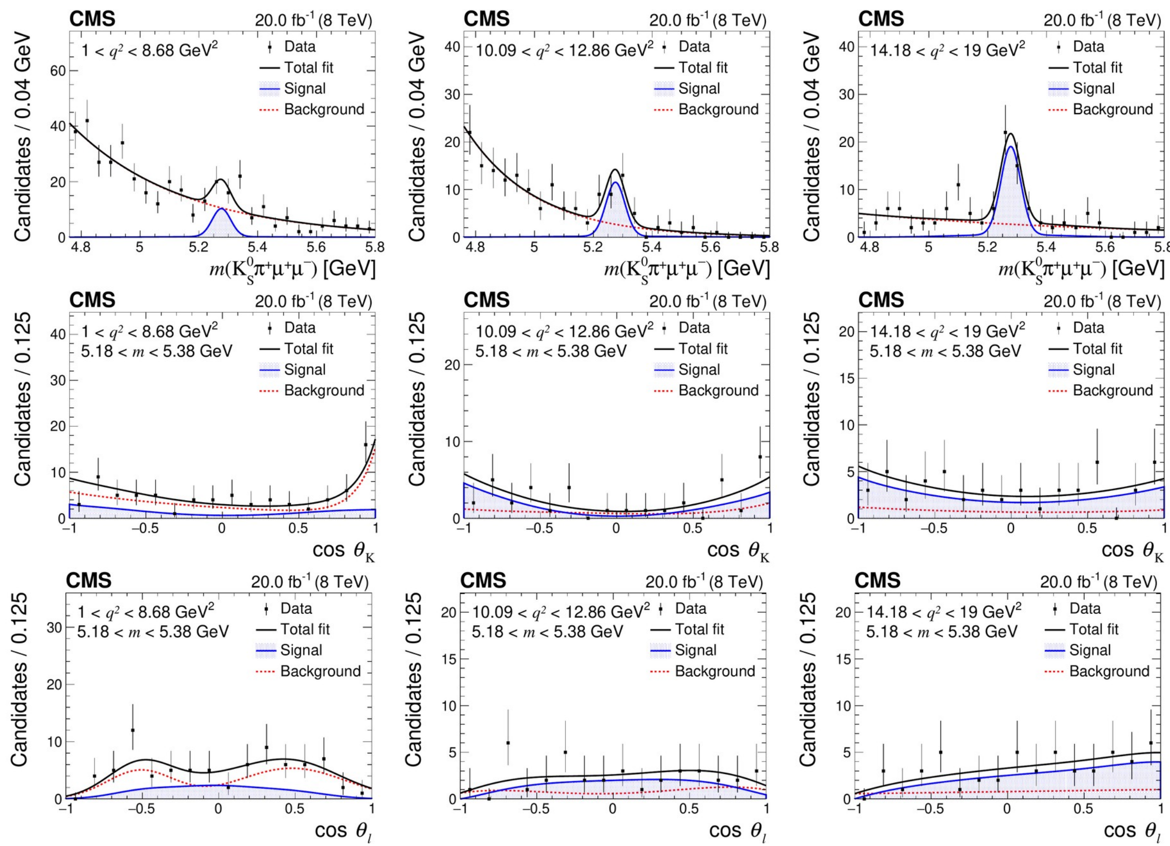

(angular projection in correspondence of peak region)

Dominant systematic uncertainties from background shape description

Source	A_{FB} (10^{-3})	F_L (10^{-3})
MC statistical uncertainty	12 – 29	18 – 38
Efficiency model	3 – 25	4 – 12
Background shape functional form	0 – 9	0 – 33
Background shape statistical uncertainty	16 – 73	20 – 87
Background shape sideband region	28 – 153	38 – 78
S-wave contamination	4 – 22	5 – 12
Total systematic uncertainty	42 – 174	55 – 127

$B^+ \to K^{*+} \mu\mu$ results

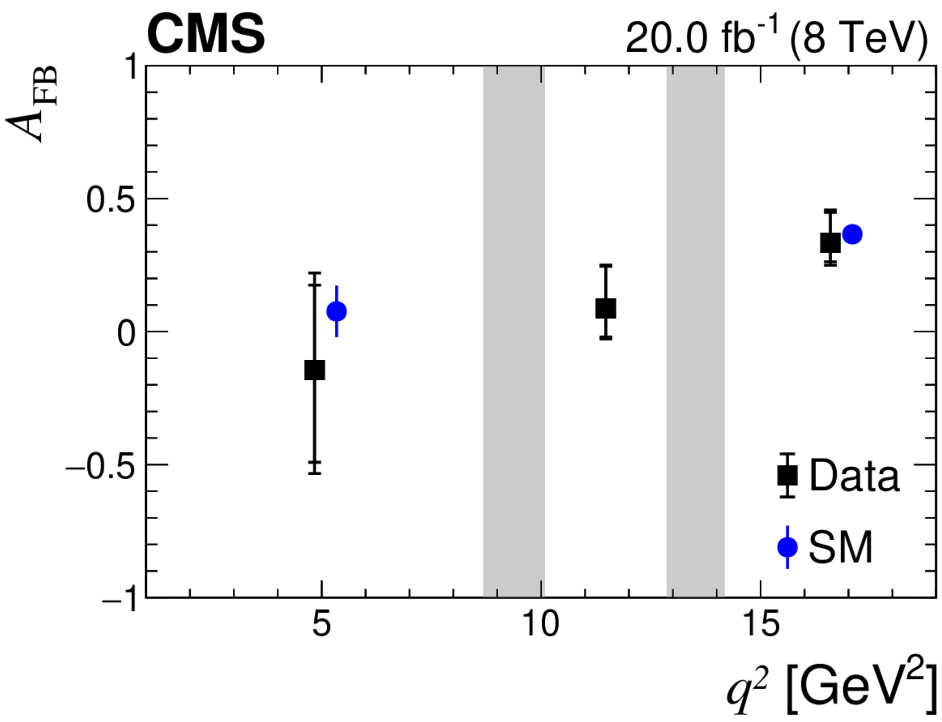

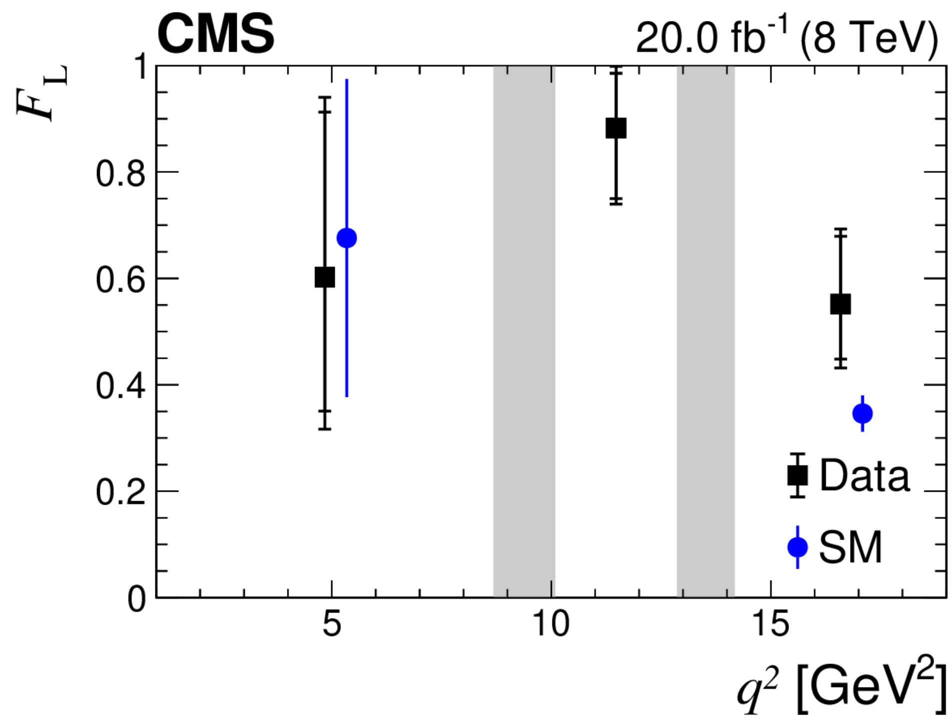

- Result dominated by statistical uncertainty (inner error bar)
- Compatible with SM predictions

Predictions from:
[JHEP 12 (2014) 125]

Prospects for $B^0 \to K^{*0} \mu\mu$ analysis at HL-LHC

[CMS-PAS-FTR-18-033]

- **Uncertainty on P'_5** from $B^0 \to K^{*0} \mu\mu$ analysis **extrapolated to HL-LHC** scenario at 3000 fb^{-1}
- Run 1 results used as baseline
- Upgraded CMS tracker detector provides improved mass resolution
- No changes in trigger performances and analysis strategy have been considered
- **Signal yield** obtained from MC simulations with Phase-2 detector upgrade and pileup of 200
  - Scaled to 3000 fb^{-1} : **~ 700k events** in the full q^2 range

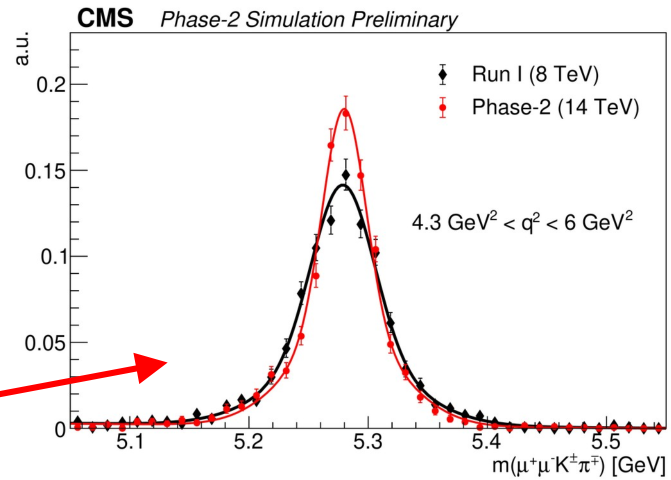

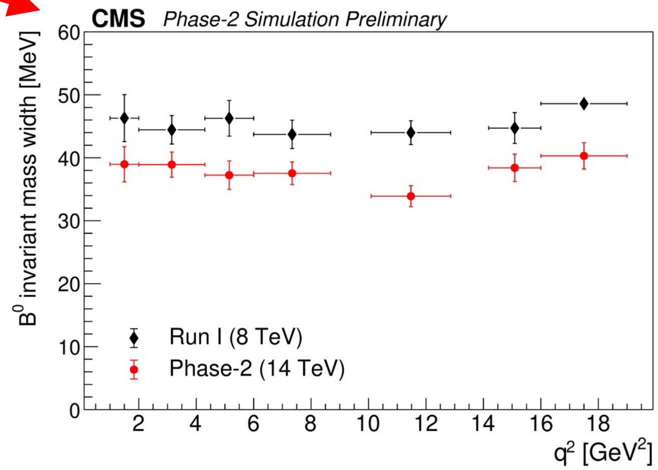

Projections on P'_5 uncertainty (HL-LHC)

- Run 1 **statistical uncertainty scaled according to the expected yield**
- Systematic uncertainties based on data control channel scaled according to statistics
- Other systematic uncertainties scaled by factor of 2
- **Total uncertainty** is expected to improve by **15 times wrt Run 1 result**
- Large signal yield allows to split q^2 range in finer bins

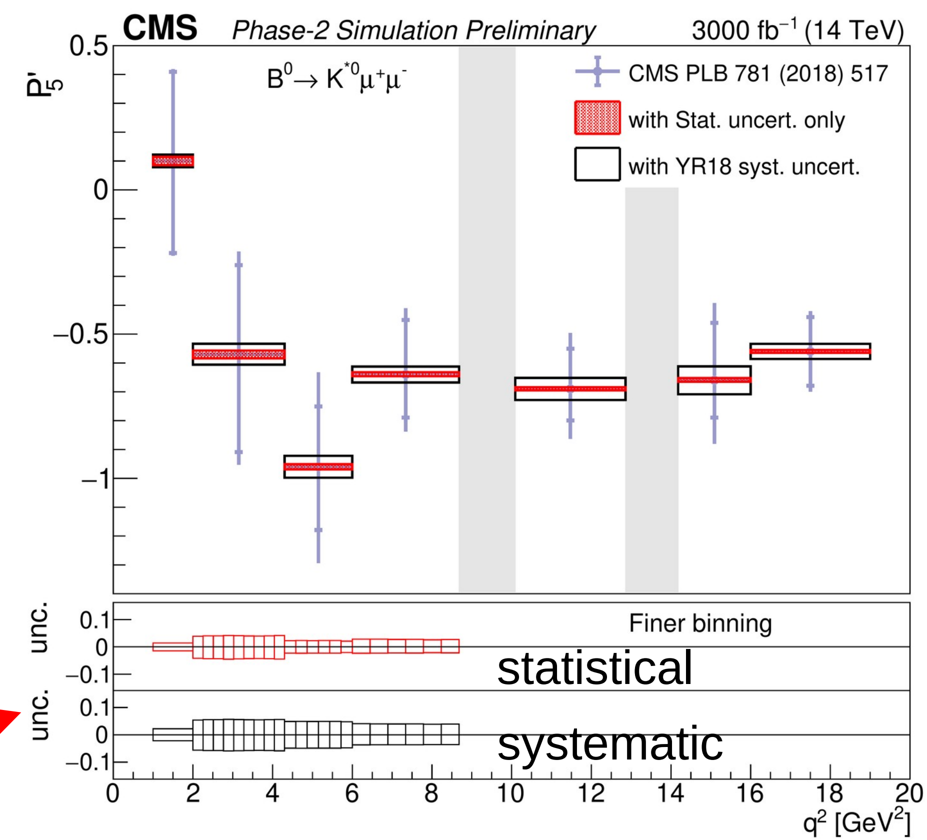

Summary and conclusions

FCNC rare decays have been extensively studied in Run 1 CMS data

- $B^0 \rightarrow K^{*0}\mu\mu$ angular analysis to measure F_L, A_{FB}, P_1 and P'_5
- $B^+ \rightarrow K^+\mu\mu$ angular analysis to measure A_{FB} and F_H
- $B^+ \rightarrow K^{*+}\mu\mu$ angular analysis to measure F_L and A_{FB}
- Prospects of $B^0 \rightarrow K^{*0}\mu\mu$ angular analysis in HL-LHC

Analyses on Run 2 data in advanced status

- dedicated trigger requiring two muons + 1 track with common vertex
- more decay channels to be explored

Stay tuned!

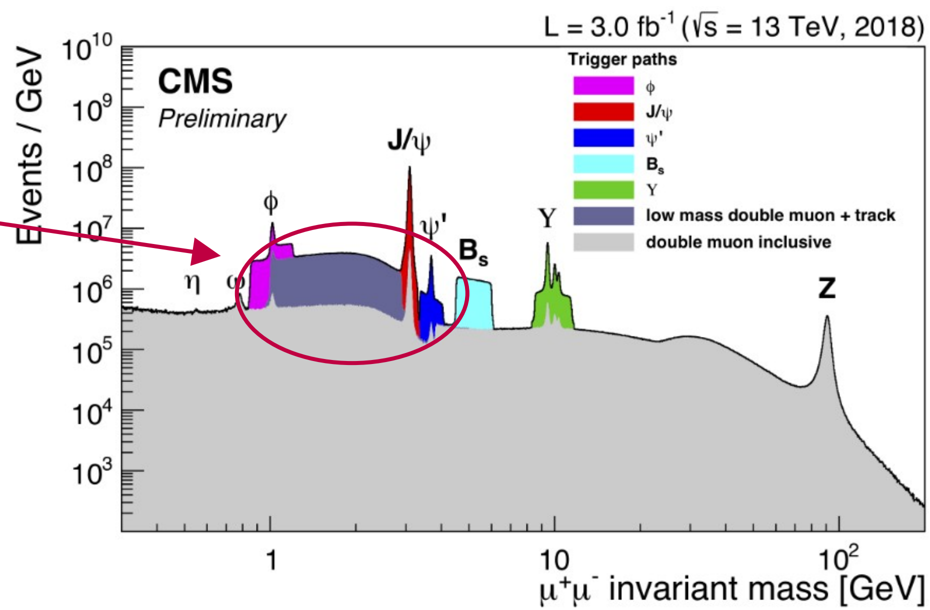

Backup

Backup ($B^0 \to K^{*0} \mu\mu$)

PDF and decay rates

Integration of ϕ angle

$$\frac{1}{\Gamma}\frac{d^3\Gamma}{d\cos\theta_K\, d\cos\theta_l\, dq^2} = \frac{9}{16}\left\{\frac{2}{3}\left[F_S + A_S\cos\theta_K\right](1-\cos^2\theta_l)\right.$$
$$+ (1-F_S)\left[2F_L\cos^2\theta_K(1-\cos^2\theta_l)\right.$$
$$+\frac{1}{2}(1-F_L)(1-\cos^2\theta_K)(1+\cos^2\theta_l)$$
$$\left.\left.+\frac{4}{3}A_{FB}(1-\cos^2\theta_K)\cos\theta_l\right]\right\}.$$

$$\begin{aligned}\mathrm{PDF}(m,\theta_K,\theta_l) = Y_S^C\Big[&S^C(m)\,S^a(\theta_K,\theta_l)\,\epsilon^C(\theta_K,\theta_l)\\ &+\frac{f^M}{1-f^M}\,S^M(m)\,S^a(-\theta_K,-\theta_l)\,\epsilon^M(\theta_K,\theta_l)\Big]\\ &+Y_B\,B^m(m)\,B^{\theta_K}(\theta_K)\,B^{\theta_l}(\theta_l),\end{aligned}$$

Folding of θ_l and ϕ angles

$$\frac{1}{d\Gamma/dq^2}\frac{d^4\Gamma}{dq^2\, d\cos\theta_\ell\, d\cos\theta_K\, d\varphi} = \frac{9}{8\pi}\left\{\frac{2}{3}\left[(F_S + A_S\cos\theta_K)(1-\cos^2\theta_\ell)\right.\right.$$
$$\left.+A_S^5\sqrt{1-\cos^2\theta_K}\sqrt{1-\cos^2\theta_\ell}\cos\varphi\right]$$
$$(1-F_S)\left[2F_L\cos^2\theta_K(1-\cos^2\theta_\ell)\right.$$
$$+\frac{1}{2}(1-F_L)(1-\cos^2\theta_K)(1+\cos^2\theta_\ell)$$
$$+\frac{1}{2}P_1(1-F_L)(1-\cos^2\theta_K)(1-\cos^2\theta_\ell)\cos 2\varphi$$
$$\left.\left.+2P_5'\cos\theta_K\sqrt{F_L(1-F_L)}\sqrt{1-\cos^2\theta_K}\sqrt{1-\cos^2\theta_\ell}\cos\varphi\right]\right\}$$

$$\begin{aligned}\mathrm{pdf}(m,\theta_K,\theta_\ell,\varphi) = Y_S^C\Big[&S^C(m)\,S^a(\theta_K,\theta_\ell,\varphi)\,\epsilon^C(\theta_K,\theta_\ell,\varphi)\\ &+\frac{f^M}{1-f^M}\,S^M(m)\,S^a(-\theta_K,-\theta_\ell,\varphi)\,\epsilon^M(\theta_K,\theta_\ell,\varphi)\Big]\\ &+Y_B\,B^m(m)\,B^{\theta_K}(\theta_K)\,B^{\theta_\ell}(\theta_\ell)\,B^{\varphi}(\varphi),\end{aligned}$$

Likelihood profiles

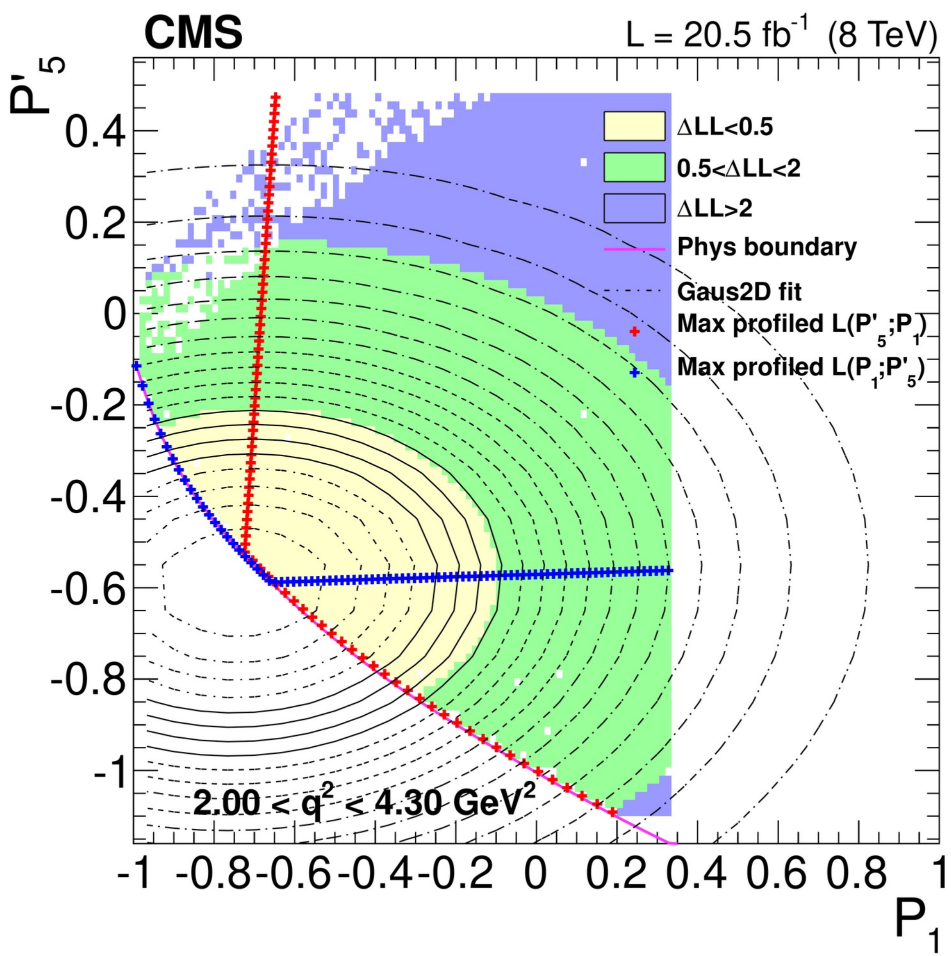

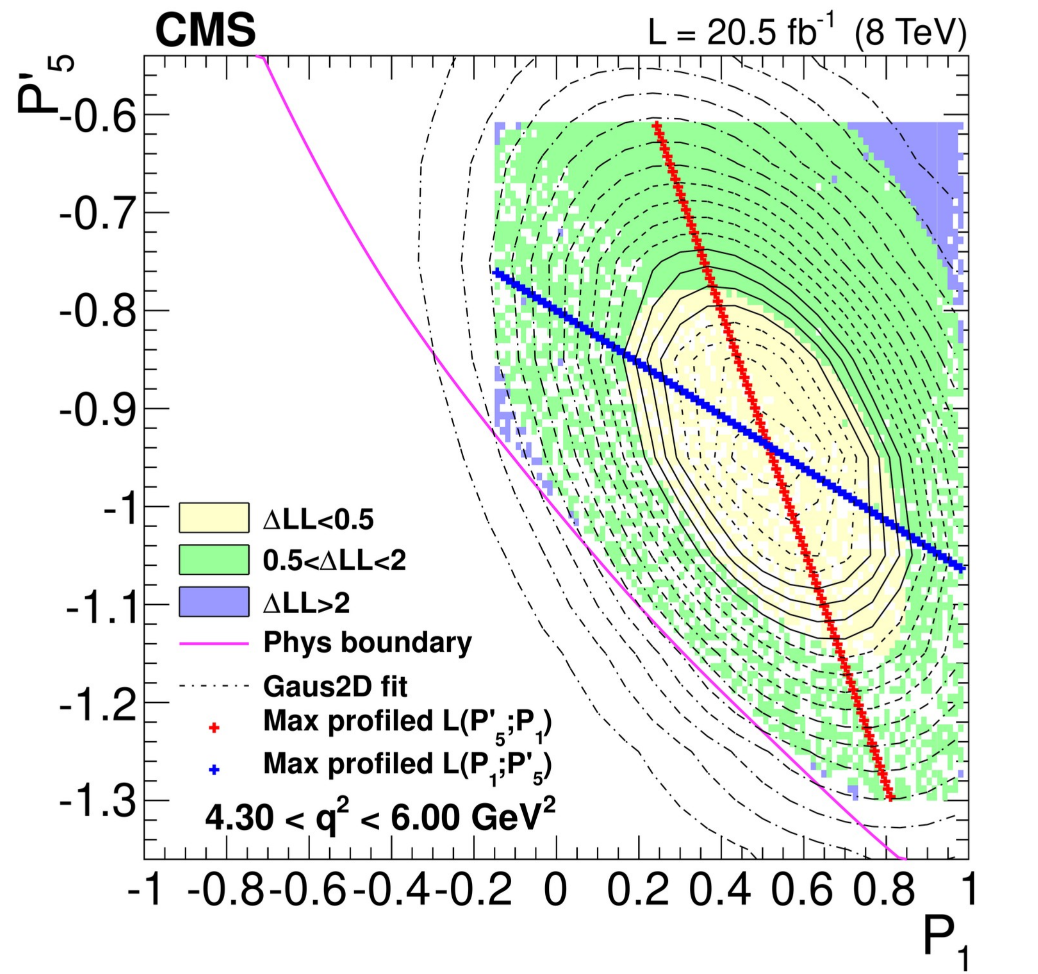

$B^0 \to K^{*0}\mu\mu$ systematics and results

Source	$P_1 (\times 10^{-3})$	$P'_5 (\times 10^{-3})$
Simulation mismodeling	1–33	10–23
Fit bias	5–78	10–120
Finite size of simulated samples	29–73	31–110
Efficiency	17–100	5–65
$K\pi$ mistagging	8–110	6–66
Background distribution	12–70	10–51
Mass distribution	12	19
Feed-through background	4–12	3–24
F_L, F_S, A_S uncertainty propagation	0–210	0–210
Angular resolution	2–68	0.1–12
Total	100–230	70–250

q^2 (GeV^2)	Signal yield	P_1	P'_5	Correlations
1.00–2.00	80 ± 12	$+0.12\ ^{+0.46}_{-0.47} \pm 0.10$	$+0.10\ ^{+0.32}_{-0.31} \pm 0.07$	-0.0526
2.00–4.30	145 ± 16	$-0.69\ ^{+0.58}_{-0.27} \pm 0.23$	$-0.57\ ^{+0.34}_{-0.31} \pm 0.18$	-0.0452
4.30–6.00	119 ± 14	$+0.53\ ^{+0.24}_{-0.33} \pm 0.19$	$-0.96\ ^{+0.22}_{-0.21} \pm 0.25$	$+0.4715$
6.00–8.68	247 ± 21	$-0.47\ ^{+0.27}_{-0.23} \pm 0.15$	$-0.64\ ^{+0.15}_{-0.19} \pm 0.13$	$+0.0761$
10.09–12.86	354 ± 23	$-0.53\ ^{+0.20}_{-0.14} \pm 0.15$	$-0.69\ ^{+0.11}_{-0.14} \pm 0.13$	$+0.6077$
14.18–16.00	213 ± 17	$-0.33\ ^{+0.24}_{-0.23} \pm 0.20$	$-0.66\ ^{+0.13}_{-0.20} \pm 0.18$	$+0.4188$
16.00–19.00	239 ± 19	$-0.53 \pm 0.19 \pm 0.16$	$-0.56 \pm 0.12 \pm 0.07$	$+0.4621$

Other results' comparisons

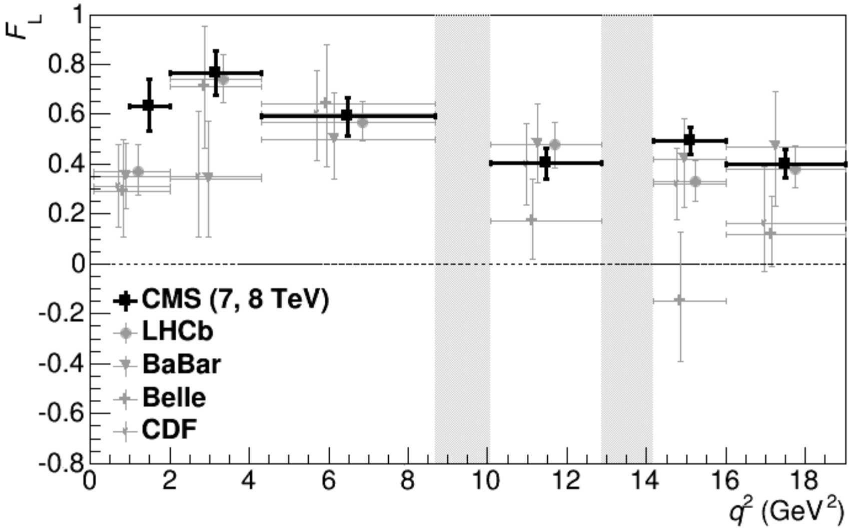

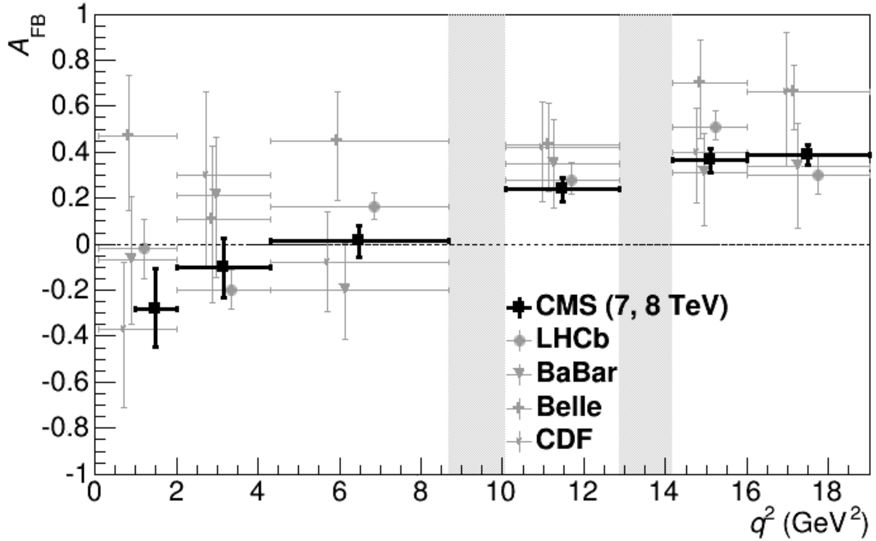

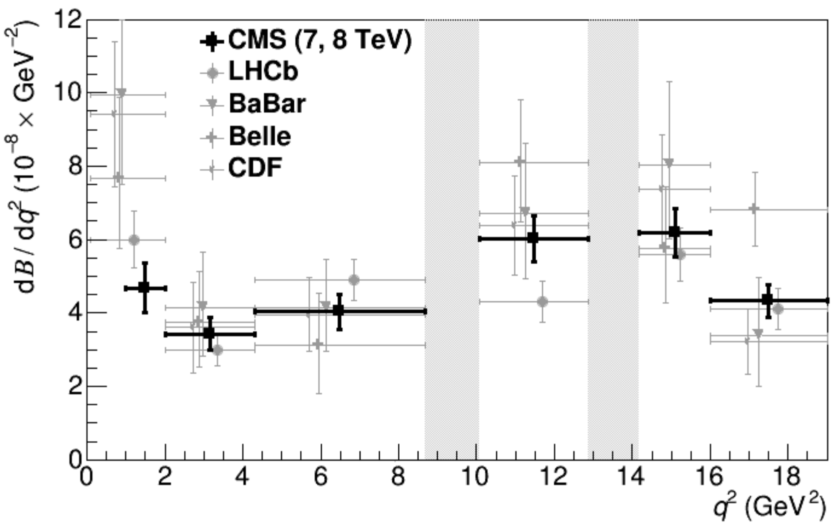

Fit projections from first analysis iteration

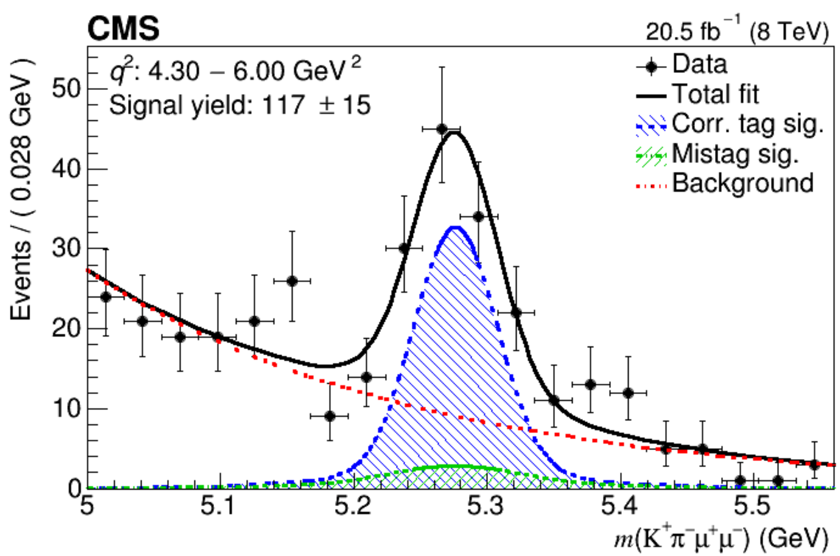

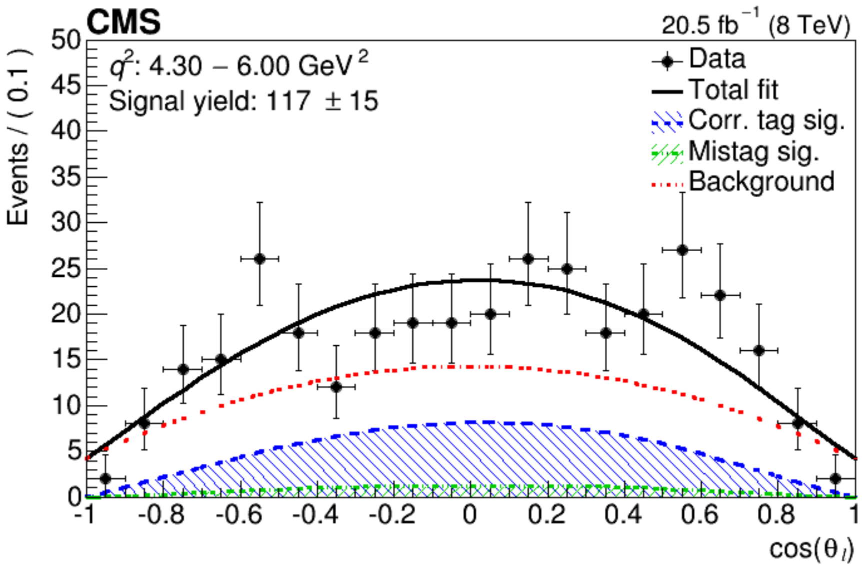

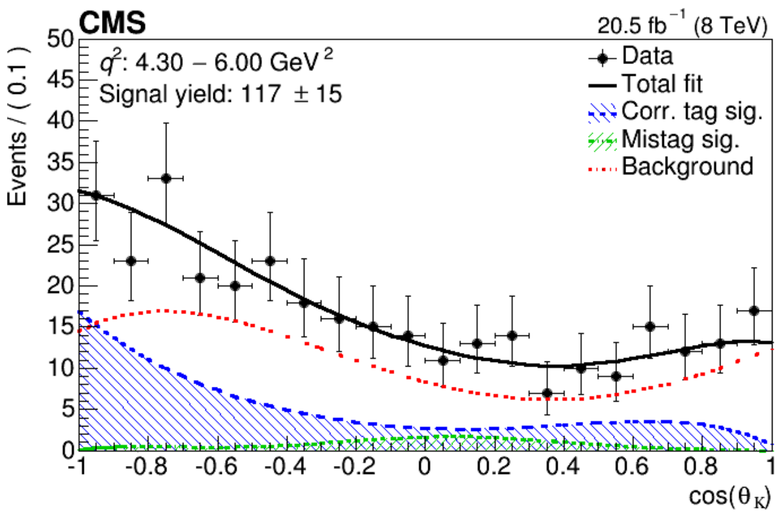

Backup ($B^+ \rightarrow K^+ \mu\mu$)

PDF and decay rate

$$\frac{1}{\Gamma_\ell}\frac{\mathrm{d}\Gamma_\ell}{\mathrm{d}\cos\theta_\ell} = \frac{3}{4}(1-F_\mathrm{H})(1-\cos^2\theta_\ell) + \frac{1}{2}F_\mathrm{H} + A_\mathrm{FB}\cos\theta_\ell.$$

$$\mathrm{pdf}(m,\cos\theta_\ell) = Y_\mathrm{S}S_\mathrm{m}(m)S_\mathrm{a}(\cos\theta_\ell)\epsilon(\cos\theta_\ell) + Y_\mathrm{B}B_\mathrm{m}(m)B_\mathrm{a}(\cos\theta_\ell),$$

Efficiency functions

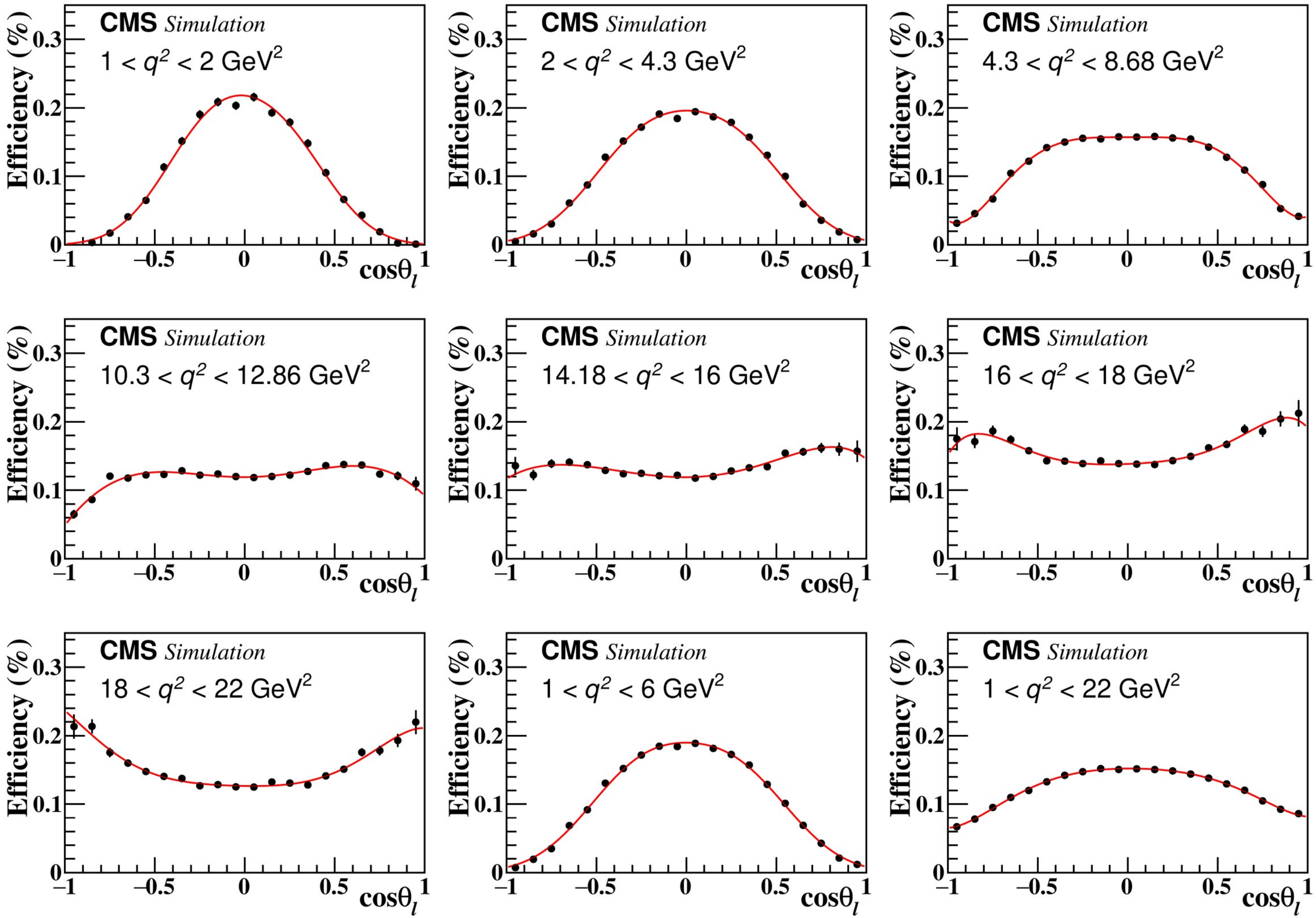

Comparison with LHCb results

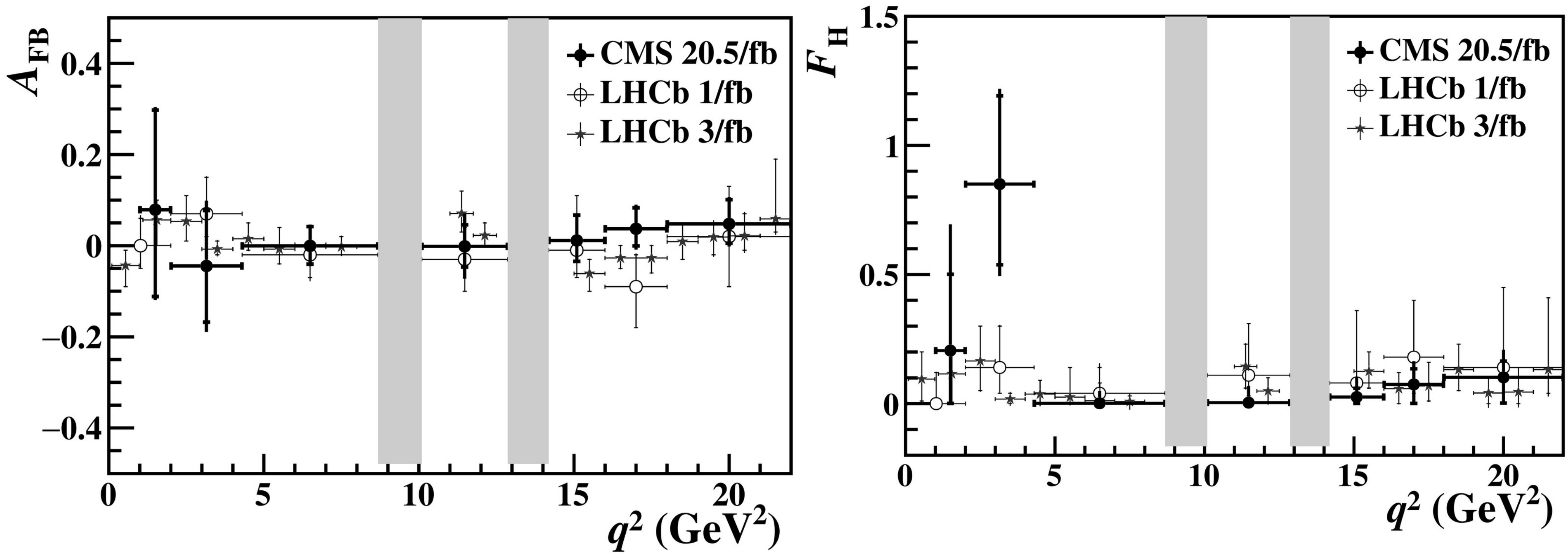

$B^+ \rightarrow K^+\mu\mu$ systematics and results

Systematic uncertainty	A_{FB} ($\times 10^{-2}$)	F_H ($\times 10^{-2}$)
Finite size of MC samples	0.4–1.8	0.9–5.0
Efficiency description	0.1–1.5	0.1–7.8
Simulation mismodeling	0.1–2.8	0.1–1.4
Background parametrization model	0.1–1.0	0.1–5.1
Angular resolution	0.1–1.7	0.1–3.3
Dimuon mass resolution	0.1–1.0	0.1–1.5
Fitting procedure	0.1–3.2	0.4–25
Background distribution	0.1–7.2	0.1–29
Total systematic uncertainty	1.6–7.5	4.4–39

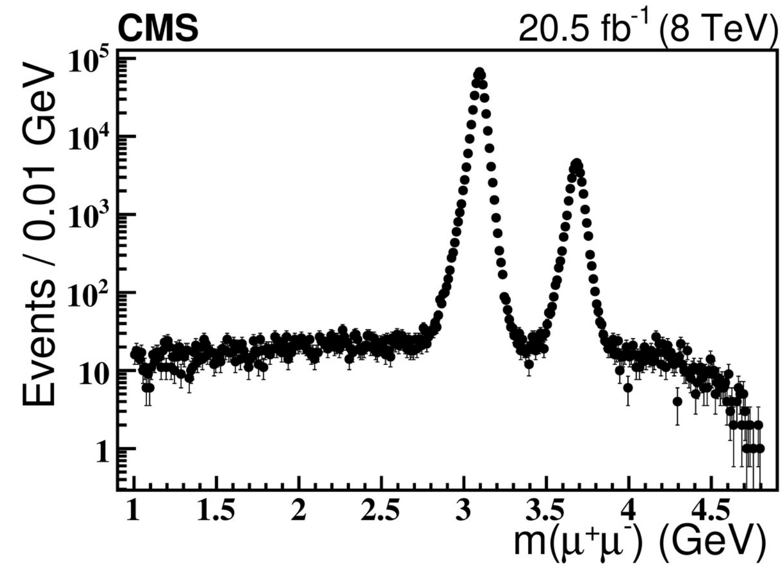

q^2 (GeV^2)	Y_S	A_{FB}	F_H	F_H(EOS)	F_H(DHMV)	F_H(FLAVIO)
1.00–2.00	169 ± 22	$0.08\,^{+0.22}_{-0.19} \pm 0.05$	$0.21\,^{+0.29}_{-0.21} \pm 0.39$	0.047	0.046	0.045
2.00–4.30	331 ± 32	$-0.04\,^{+0.12}_{-0.12} \pm 0.07$	$0.85\,^{+0.34}_{-0.31} \pm 0.14$	0.024	0.023	0.022
4.30–8.68	785 ± 42	$0.00\,^{+0.04}_{-0.04} \pm 0.02$	$0.01\,^{+0.02}_{-0.01} \pm 0.04$	—	0.012	0.011
10.09–12.86	365 ± 29	$0.00\,^{+0.05}_{-0.05} \pm 0.05$	$0.01\,^{+0.02}_{-0.01} \pm 0.06$	—	—	—
14.18–16.00	215 ± 19	$0.01\,^{+0.06}_{-0.05} \pm 0.02$	$0.03\,^{+0.03}_{-0.03} \pm 0.07$	0.007	0.007	0.006
16.00–18.00	262 ± 21	$0.04\,^{+0.05}_{-0.04} \pm 0.03$	$0.07\,^{+0.06}_{-0.07} \pm 0.07$	0.007	0.007	0.006
18.00–22.00	226 ± 20	$0.05\,^{+0.05}_{-0.04} \pm 0.02$	$0.10\,^{+0.06}_{-0.10} \pm 0.09$	0.008	0.009	0.008
1.00–6.00	778 ± 47	$-0.14\,^{+0.07}_{-0.06} \pm 0.03$	$0.38\,^{+0.17}_{-0.21} \pm 0.09$	0.025	0.025	0.020
1.00–22.00	2286 ± 73	$0.00\,^{+0.02}_{-0.02} \pm 0.03$	$0.01\,^{+0.01}_{-0.01} \pm 0.06$	—	—	—

Backup ($B^+ \to K^{*+} \mu\mu$)

$B^+ \to K^{*+}\mu\mu$ angular distribution

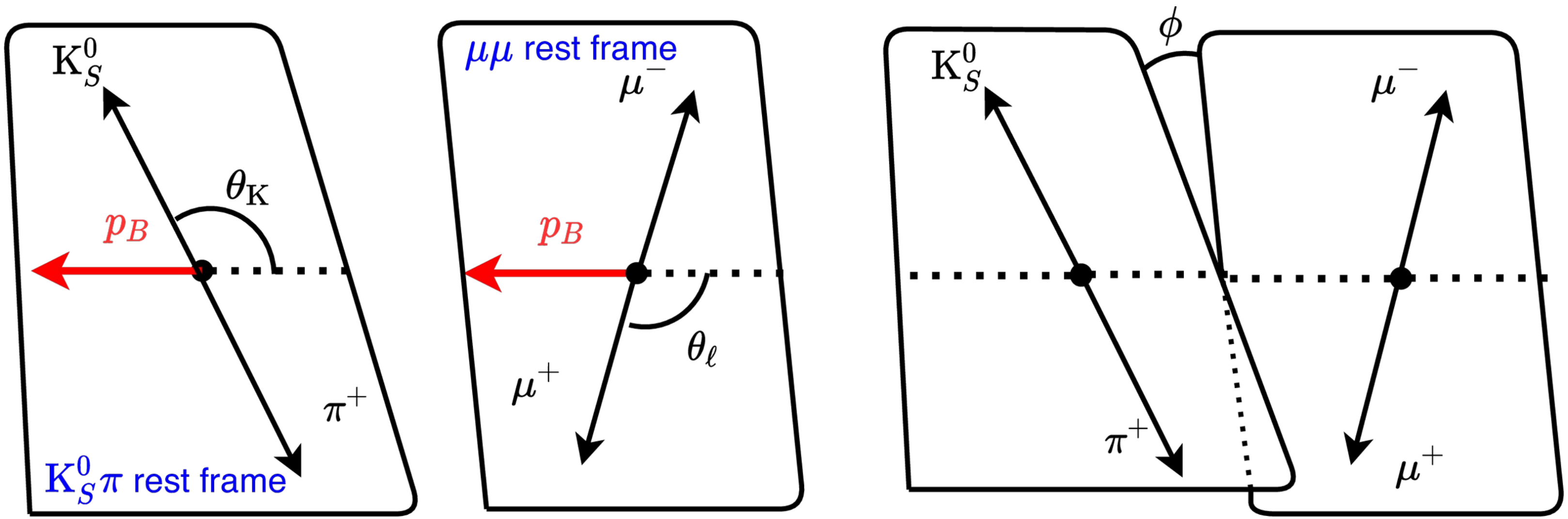

$$\frac{1}{\Gamma}\frac{\mathrm{d}^3\Gamma}{\mathrm{d}\cos\theta_K\,\mathrm{d}\cos\theta_\ell\,\mathrm{d}q^2} = \frac{9}{16}\left\{\frac{2}{3}\left[F_S + 2A_S\cos\theta_K\right]\left(1-\cos^2\theta_\ell\right)\right.$$
$$+\ (1-F_S)\left[2F_L\cos^2\theta_K\left(1-\cos^2\theta_\ell\right)\right.$$
$$+\ \frac{1}{2}(1-F_L)\left(1-\cos^2\theta_K\right)\left(1+\cos^2\theta_\ell\right)$$
$$\left.\left.+\ \frac{4}{3}A_{FB}\left(1-\cos^2\theta_K\right)\cos\theta_\ell\right]\right\}.$$

$B^+ \to K^{*+}\mu\mu$ efficiency

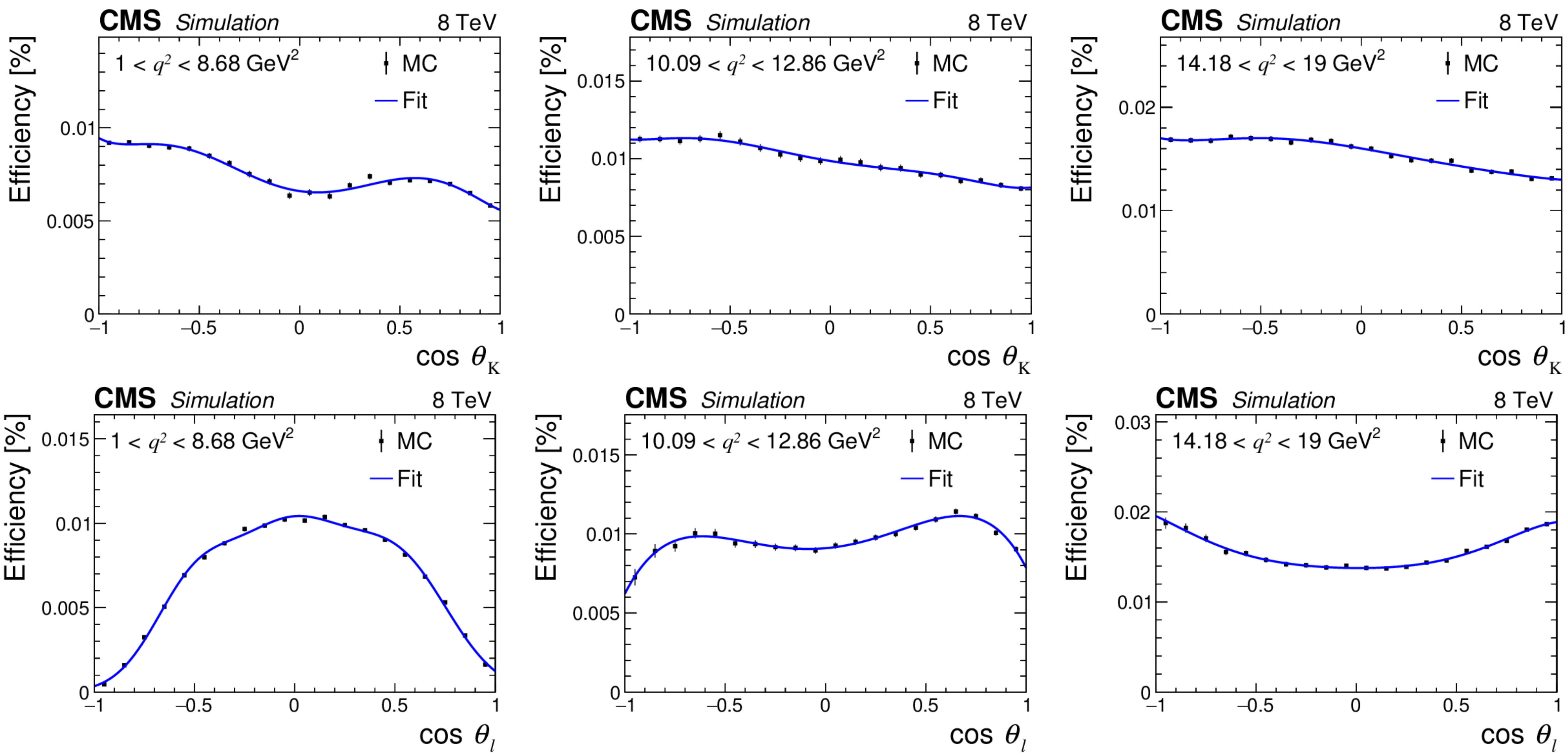

$B^+ \to K^{*+}\mu\mu$ fit projections

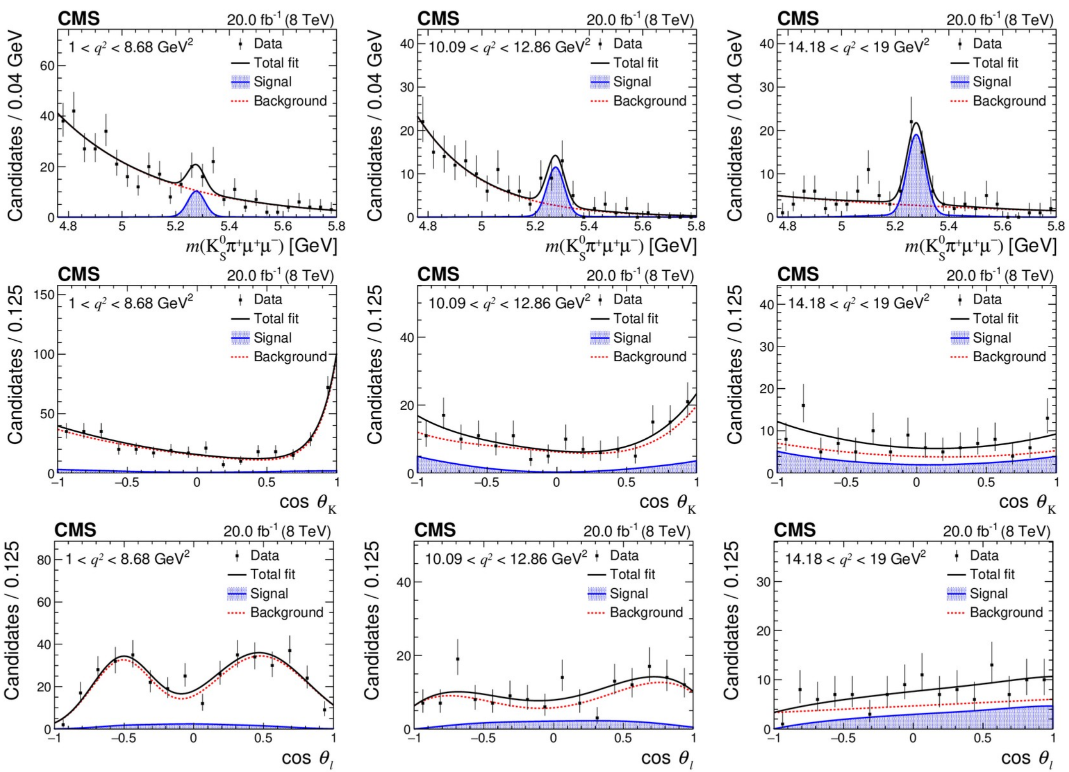

Projections in full mass range

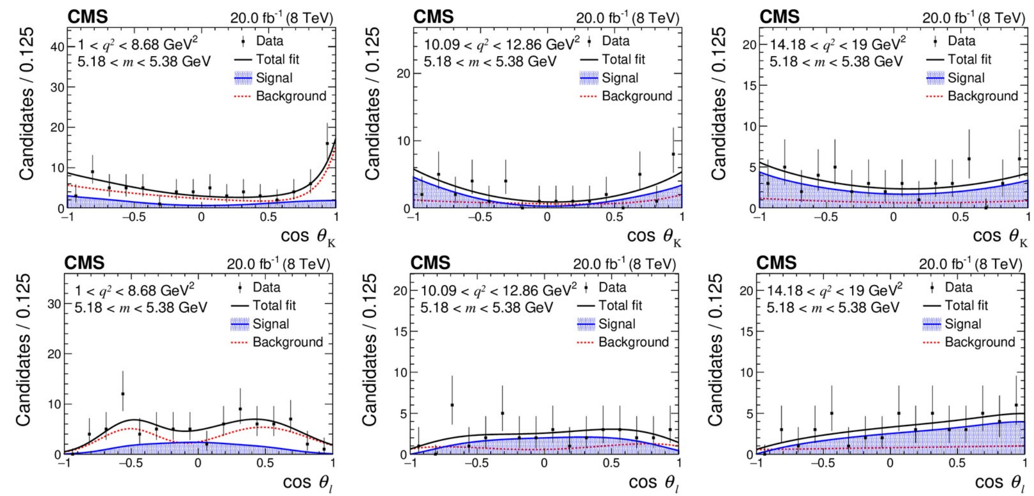

Projections in peak region

$B^+ \to K^{*+}\mu\mu$ systematics and results

Source	A_{FB} (10^{-3})	F_L (10^{-3})
MC statistical uncertainty	12 – 29	18 – 38
Efficiency model	3 – 25	4 – 12
Background shape functional form	0 – 9	0 – 33
Background shape statistical uncertainty	16 – 73	20 – 87
Background shape sideband region	28 – 153	38 – 78
S-wave contamination	4 – 22	5 – 12
Total systematic uncertainty	42 – 174	55 – 127

q^2 (GeV^2)	Y_S	A_{FB}	F_L
1 – 8.68	22.1 ± 8.1	$-0.14\,^{+0.32}_{-0.35} \pm 0.17$	$0.60\,^{+0.31}_{-0.25} \pm 0.13$
10.09 – 12.86	25.9 ± 6.3	$0.09\,^{+0.16}_{-0.11} \pm 0.04$	$0.88\,^{+0.10}_{-0.13} \pm 0.05$
14.18 – 19	45.1 ± 8.0	$0.33\,^{+0.11}_{-0.07} \pm 0.05$	$0.55\,^{+0.13}_{-0.10} \pm 0.06$